

1 **Title:** Common ancestry of heterodimerizing TALE homeobox transcription factors across  
2 Metazoa and Archaeplastida

3

4 **Short title:** Origins of TALE transcription factor networks

5

6 Sunjoo Joo<sup>1,5</sup>, Ming Hsiu Wang<sup>1,5</sup>, Gary Lui<sup>1</sup>, Jenny Lee<sup>1</sup>, Andrew Barnas<sup>1</sup>, Eunsoo Kim<sup>2</sup>,  
7 Sebastian Sudek<sup>3</sup>, Alexandra Z. Worden<sup>3</sup>, and Jae-Hyeok Lee<sup>1,4†</sup>

8

9 1. Department of Botany, University of British Columbia, 6270 University Blvd., Vancouver,  
10 BC V6T 1Z4, Canada

11 2. Division of Invertebrate Zoology and Sackler Institute for Comparative Genomics,  
12 American Museum of Natural History, 200 Central Park West, New York, NY 10024, United  
13 States

14 3. Monterey Bay Aquarium Research Institute, 7700 Sandholdt Rd., Moss Landing, CA  
15 95039, United States

16 4. Corresponding author

17 5. Equally contributed

18

19 Corresponding Author:

20 Jae-Hyeok Lee

21 #2327-6270 University Blvd.

22 1-604-827-5973

23 [jae-hyeok.lee@botany.ubc.ca](mailto:jae-hyeok.lee@botany.ubc.ca)

24

25 **Abstract**

26

27 Homeobox transcription factors (TFs) in the TALE superclass are deeply embedded in the  
28 gene regulatory networks that orchestrate embryogenesis. Knotted-like homeobox (KNOX)  
29 TFs, homologous to animal MEIS, have been found to drive the haploid-to-diploid transition  
30 in both unicellular green algae and land plants via heterodimerization with other TALE  
31 superclass TFs, representing remarkable functional conservation of a developmental TF  
32 across lineages that diverged one billion years ago. To delineate the ancestry of TALE-TALE  
33 heterodimerization, we analyzed TALE endowment in the algal radiations of Archaeplastida,  
34 ancestral to land plants. Homeodomain phylogeny and bioinformatics analysis partitioned  
35 TALEs into two broad groups, KNOX and non-KNOX. Each group shares previously defined  
36 heterodimerization domains, plant KNOX-homology in the KNOX group and animal PBC-  
37 homology in the non-KNOX group, indicating their deep ancestry. Protein-protein interaction  
38 experiments showed that the TALEs in the two groups all participated in heterodimerization.  
39 These results indicate that the TF dyads consisting of KNOX/MEIS and PBC-containing  
40 TALEs must have evolved early in eukaryotic evolution, a likely function being to accurately  
41 execute the haploid-to-diploid transitions during sexual development.

42

43 **Author summary**

44 Complex multicellularity requires elaborate developmental mechanisms, often based on the  
45 versatility of heterodimeric transcription factor (TF) interactions. Highly conserved TALE-  
46 superclass homeobox TF networks in major eukaryotic lineages suggest deep ancestry of  
47 developmental mechanisms. Our results support the hypothesis that in early eukaryotes, the  
48 TALE heterodimeric configuration provided transcription-on switches via dimerization-  
49 dependent subcellular localization, ensuring execution of the haploid-to-diploid transition  
50 only when the gamete fusion is correctly executed between appropriate partner gametes, a  
51 system that then diversified in the several lineages that engage in complex multicellular  
52 organization.

53

54 **Keywords:** Archaeplastida evolution; developmental mechanism; KNOX transcription factor;  
55 PBC-homology; TALE-class homeobox; transcription factor heterodimerization

56

## 57 Introduction

58

59 The homeobox transcription factors (TFs) are ubiquitous in eukaryotes, carrying a DNA-  
60 binding homeodomain typically 60 amino acids, that folds into three  $\alpha$ -helices [1]. The  
61 atypical or TALE (Three Amino acid Length Extension) superclass of homeobox TFs shares  
62 a three-amino-acid insertion between helix 1 and 2 and plays essential roles during  
63 embryonic development by participating in interactive TF networks. In animals, MEIS- and  
64 PBC-class TALE proteins, such as Meis/Hth and Pbx/Exd, form heterodimers that in turn  
65 form ternary complexes with HOX-class homeobox TFs, determining cellular fates along the  
66 anterior-posterior axis of the developing embryo [2,3]. In plants, the interacting KNOX- and  
67 BELL-class TFs in the TALE group play critical roles during organ formation and the  
68 vegetative-to-reproductive transition in the undifferentiated cell mass known as the shoot  
69 apical meristem [4,5].

70

71 The heterodimerization of TALE proteins serves as a trigger for precise execution of  
72 developmental programs. Prior to heterodimerization, animal PBX proteins are localized in  
73 the cytosol, and upon binding to MEIS, they translocate to the nucleus [6,7]. Similar  
74 heterodimerization-dependent translocation is also observed for KNOX-BELL pairs in the  
75 plant *Arabidopsis*, implying that this mechanism is a conserved regulatory feature of TALE  
76 proteins [8]. In addition, TALE proteins differ in their DNA-binding specificity [9,10], which is  
77 primarily determined by the homeodomain residues at positions 47, 50, and 54 [11], and  
78 heterodimerization increases target affinity by bringing two such DNA-binding domains  
79 together.

80

81 TALE-heterodimerization is mediated by class-specific homology domains located on the N-  
82 terminal side adjacent to the homeodomain [12,13]. Animal MEIS and plant KNOX class  
83 proteins share readily identifiable homology in their heterodimerization domain, leading to  
84 the proposal of an ancestral TALE class named MEINOX [12]. In contrast, their partner  
85 classes -- PBC and BELL -- exhibit no apparent homology in their heterodimerization  
86 domains. Short shared sequence motifs and common secondary structures have been found  
87 within the heterodimerization domains between MEINOX and PBC or BELL [14,15], but their  
88 extent of the homology requires adequate taxon sampling to recover ancestral relationships.

89

90 An ancestral functions of TALE-TALE heterodimerization was revealed in studies of the  
91 unicellular green alga *Chlamydomonas reinhardtii*: the KNOX ortholog GSM1 and a second  
92 TALE protein GSP1 form heterodimers immediately after the fusion of sexual gametes, and

93 these drive the haploid-to-diploid transition by activating >200 diploid-specific genes and  
94 inactivating >100 haploid-specific genes [10,16,17]. In subsequent studies, plant-type TALE-  
95 TALE heterodimers between KNOX and BELL were shown to be required for the haploid-to-  
96 diploid transition of the moss *Physcomitrella patens* [18,19]. Given the conserved role of  
97 TALE heterodimerization as a developmental switch in the sexual life cycle of the plant  
98 lineage, understanding its origins and diversification promises to shed light on the evolution  
99 of developmental mechanisms during eukaryotic radiation and the emergence of land plants.

100

101 To delineate the ancestry of plant-type TALE heterodimerization, we performed a  
102 phylogenetic and bioinformatics analysis of TALE TFs in the three algal radiations of the  
103 Archaeplastida supergroup, the descendants of a single endosymbiosis event > one billion  
104 years ago [20,21]. Our analysis showed that the TALEs were already diversified into two  
105 groups at the origin of Archaeplastida, one sharing KNOX-homology and the other sharing  
106 PBC-homology. Together with our protein-protein interaction data, we propose that all TALE  
107 classes participate in heterodimerization networks via the KNOX- and PBC-homology  
108 domains between the two ancestral groups.

109

## 110 **Results**

111

### 112 **TALEs in Archaeplastida are divided into two groups, KNOX and non-KNOX**

113 The Archaeplastida consists of three monophyletic phyla [22,23] (Fig 1). 1) Viridiplantae  
114 include two divisions, Chlorophyta -- chlorophytes and prasinophytes (a paraphyletic group  
115 of seven lineages [24]) -- and Streptophyta -- charophyte algae and land plants [25]. 2)  
116 Rhodophyta (red algae) include diverse unicellular and multicellular organisms that diverge  
117 into four major lineages [26] (S1 Spreadsheet). 3) Glaucophyta members include only four  
118 cultured genera and possess plastids that carry ancestral features of the cyanobacterial  
119 symbiont that gave rise to photosynthetic organelles in eukaryotes [27].

120

121 To collect all the available homeobox protein sequences, we performed BLAST and Pfam-  
122 motif searches against non-plant genomes and transcriptome assemblies throughout the  
123 Archaeplastida (S1 Spreadsheet), identifying 327 proteins from 55 species as the  
124 Archaeplastida homeobox collection (29 genomes and 18 transcriptomes; S2 Spreadsheet).  
125 Of these, 102 possessed the defining feature of TALE proteins, a three-amino-acid insertion  
126 between aa positions 23-24 in the homeodomain [28]. At least two TALE genes were  
127 detected in most genomes except five genomes in the Trebouxiophyceae class of the  
128 Chlorophyta (S1 Spreadsheet; see S1A Notes for further discussion of the absence of  
129 TALEs in Trebouxiophyceae).

130

131 The collected TALE sequences were then classified by their homeodomain features using a  
132 phylogenetic approach, with TALEs from animals, plants, and early-diverging eukaryotes  
133 (Amoebozoa and Excavata) as outgroups (S1 Fig). The resultant TALE homeodomain  
134 phylogeny distinguished two groups in all three phyla of Archaeplastida (Fig 2). 1) The  
135 KNOX-group as a well-supported clade displayed a phylum-specific cladogram: two  
136 Glaucophyta sequences at the base (as KNOX-Glauco) were separate from the next clade,  
137 which combines Rhodophyta sequences (as KNOX-Red1) and a Viridiplantae-specific clade  
138 with strong support (92/90/1.00). 2) The non-KNOX group, including the BELL and GSP1  
139 homologs, contained clades of mixed taxonomic affiliations. These analyses showed that the  
140 TALE proteins had already diverged into two groups before the evolution of the  
141 Archaeplastida and that the KNOX-group is highly conserved throughout Archaeplastida.

142

#### 143 **KNOX group sequences share the same heterodimerization domains throughout** 144 **Archaeplastida**

145 The next question was whether the plant KNOX class originated prior to the Viridiplantae  
146 phylum. The plant KNOX proteins and the Chlorophyta GSM1 possess KNOX-homology  
147 sequences, consisting of KN-A, KN-B and ELK domains, required for their  
148 heterodimerization with other TALE proteins [10]; therefore, the presence of the KNOX  
149 homology sequences suggest functional homology to the plant KNOX class. To collect  
150 homology domains without prior information, we performed ad-hoc homology domain  
151 searches among the KNOX group sequences. Using the identified homology domains as  
152 anchors, we carefully curated an alignment of the KNOX-group sequences combined with  
153 any other TALE sequences with a KNOX-homology, (S2 Fig). From this KNOX alignment,  
154 we defined KNOX-homologs as having amino acid similarity scores >50% for at least two of  
155 the three domains comprising the KNOX-homology region (S3 Spreadsheet for calculated  
156 domain homology). Using this criterion, all KNOX group sequences (excluding partial  
157 sequences) possessed the KNOX homology (Fig 2, marked by red dots following their IDs),  
158 indicating that the KNOX-homolog already existed before the evolution of eukaryotic  
159 photosynthesis as represented by the Archaeplastida.

160

161 In addition to the KNOX-homology, the same search also revealed two novel domains at the  
162 C-terminus of the homeodomain (S2 Fig): the first (KN-C1) was shared among the  
163 Chlorophyta sequences, and the second (KN-C2) was shared among a group of KNOX  
164 homologs in a clade outside the KNOX-group (KNOX-Red2).

165

#### 166 **KNOX classes diverged independently among the algal phyla**

167 In Viridiplantae, we found a single KNOX homolog in most Chlorophyta species, whereas  
168 KNOX1 and KNOX2 divergence was evident in the Streptophyta division, including the  
169 charophyte *Klebsormidium flaccidum* and land plants (Fig 2). The newly discovered KN-C1  
170 domain was specific to the Chlorophyta KNOX sequences and found in all but one species  
171 (*Pyramimonas amyliifera*). The absence of similarity between KN-C1 and the C-terminal  
172 extensions of KNOX1/KNOX2 sequences suggests independent, lineage-specific KNOX  
173 evolution in the Chlorophyta and Streptophyta (S2 Fig). We, therefore, refer to the  
174 Chlorophyta KNOX classes as KNOX-Chloro in contrast to the KNOX1 and KNOX2 classes  
175 in the Streptophyta.

176  
177 The KNOX homologs in the Rhodophyta were divided into two classes: a paraphyletic group  
178 close to the KNOX-Chloro clade, named KNOX-Red1, and a second group near the PBX-  
179 Outgroup, named KNOX-Red2. KNOX-Red1 lacked a KN-A, whereas KNOX-Red2 lacked  
180 an ELK and shared a KN-C2 domain (S2 Fig). We consider KNOX-Red1 as the ancestral  
181 type, since the KNOX-Red1 sequences were found in all examined Rhodophyta taxa,  
182 whereas the KNOX-Red2 sequences were restricted to two taxonomic classes  
183 (Cyanidiophyceae and Florideophyceae). Interestingly, the KNOX-Red2 clade included two  
184 green algal sequences, with strong statistical support (89/89/0.97; Fig 2); these possessed a  
185 KN-C2 domain, suggesting their ancestry within the KNOX-Red2 class (S2 Fig; see S1B  
186 Notes for further discussion about their possible origin via horizontal gene transfer).

187  
188 Available TALE sequences were limited for the Glaucophyta. We found a single KNOX  
189 homolog in two species, which possessed KN-A and KN-B domains but lacked an ELK  
190 domain. We termed these KNOX-Glauco.

191  
192 **Non-KNOX group TALEs possess animal type PBC-homology domain, suggesting a**  
193 **shared ancestry between Archaeplastida and Metazoa**

194 Following the identification of KNOX homologs, the non-KNOX group in the Archaeplastida  
195 was redefined as lacking KN-A and KN-B domains. Further classification of the non-KNOX  
196 group was challenging due to its highly divergent homeodomain sequences. However, we  
197 noticed that the number of non-KNOX genes per species was largely invariable: one in most  
198 Rhodophyta and Glaucophyta genomes and two in the majority of Chlorophyta genomes,  
199 suggesting their conservation within each radiation.

200  
201 Our ad-hoc homology search provided critical information for non-KNOX classification,  
202 identifying a homology domain shared among all Glaucophyta and Rhodophyta non-KNOX  
203 sequences (Fig 3A and 3B). Since this domain showed a similarity to the second half of the

204 animal PBC-B domain (Pfam ID: PF03792) known as heterodimerization domain [12], we  
205 named this domain PBL (PBC-B Like). Accordingly, we classified all the non-KNOX TALEs  
206 in Glaucophyta and Rhodophyta as a single PBC-related homeobox class, PBX-Glauco or  
207 PBX-Red. PBX-Glauco sequences also possessed the MEIONOX motif, conserved in the  
208 animal PBC-B domain, indicating common ancestry of PBC-B and PBL domains (Fig 3A).

209

### 210 **GSP1 shares distant PBC-homology together with other non-KNOX group sequences** 211 **in Viridiplantae**

212 A remaining question was the evolution of the Chlorophyta non-KNOX sequences that  
213 apparently lacked a PBC-homology. To uncover even a distant homology, we compared the  
214 newly defined PBL domains with the Chlorophyta sequences by BLAST (cut-off E-value of  
215 1E-1) and multiple sequence alignments. This query collected three prasinophyte and one  
216 charophyte TALE sequences that possessed a MEINOX motif and a putative PBL-domain;  
217 however, they showed very low sequence identity among themselves (Fig 3C). Further  
218 query utilizing these four sequences identified 11 additional non-KNOX sequences. Nine of  
219 these were made into two alignments, one including GSP1 homologs and the other  
220 combining most prasinophyte sequences (S3A and S3B Fig). The two remaining sequences  
221 (*Picocystis\_salinarum\_04995* and *Klebsormidium\_flaccidum\_00021\_0250*) showed a  
222 homology to a PBX-Red sequence of *Chondrus cruentum* (ID:41034) in a ~ 200 aa-long  
223 extension beyond the PBL domain, suggesting their PBX-Red ancestry (another potential  
224 case of horizontal transfers; S4 Fig). All the Chlorophyta non-KNOX sequences that carry  
225 the PBL-homology domains were classified as GLX (GSP1-like homeobox) in recognition of  
226 the GSP1 protein of *Chlamydomonas* as the first characterized member of this class [29].

227

### 228 **Two non-KNOX paralogs of Chlorophyta heterodimerize with the KNOX homologs.**

229 Even with our sensitive iterative homology search, we could not identify a PBC/PBL-  
230 homology in about half of the Chlorophyta non-KNOX sequences. Since most Chlorophyta  
231 genomes possess one GLX homolog and one non-KNOX sequence without the PBL-  
232 homology domain, we refer the latter collectively to Class-B (S5 Fig). Exceptions were found  
233 in one prasinophyte clade (class Mamiellophyceae), whose six high-quality genomes all  
234 contain two non-KNOX sequences lacking the PBL-homology. Nonetheless, these non-  
235 KNOX sequences formed two groups, one more conserved and the other less conserved,  
236 referred to the Mam-A and Mam-B classes, respectively (S6 and S7 Fig). Considering the  
237 reductive genome evolution of the Mamiellophyceae [30], the conserved Mam-A class may  
238 be derived from an ancestral GLX class.

239

240 Two divergent non-KNOX classes in Chlorophyta led to a critical question about their dyadic  
241 networks. Previously studies had shown that TALE heterodimers required interaction  
242 between MEIS and PBC domains in animals and between KNOX and PBL domains in  
243 *Chlamydomonas* [6,10]. It was, therefore, predicted that all Glaucophyta and Rhodophyta  
244 TALEs form heterodimers via their KNOX- and PBL-homology domains. On the other hand,  
245 it remained to be tested whether the Chlorophyta TALEs lacking a PBL-domain can form  
246 heterodimers with other TALEs.

247

248 To characterize interaction network of TALE class proteins in Chlorophyta, we selected three  
249 prasinophyte species for protein-protein interaction assays: two species containing Mam-A  
250 and Mam-B genes (*Micromonas commoda* and *Ostreococcus tauri*), and another species  
251 (*Picocystis salinarum*), whose transcriptome contained one GLX and one Class-B sequence.  
252 In all three species, we found that KNOX homologs interacted with all examined non-KNOX  
253 proteins in Mam-A, Mam-B, Class-B, and GLX class (Fig 4A-4C). No interaction was  
254 observed between the two non-KNOX proteins in any of the three species (Fig 4A-4C).  
255 Similar to the GLX-KNOX heterodimerization, Mam-A and Mam-B also required additional  
256 domains outside the homeodomain for their heterodimerization with the KNOX homologs  
257 (S8 Fig). These results showed that the all divergent non-KNOX TALEs maintained their  
258 original activity to form heterodimers with the KNOX homologs. Observed interacting  
259 network among the TALE sequences is summarized in S9A Fig.

260

### 261 **TALE heterodimerization evolved early in eukaryotic history**

262 Our discovery of the PBC-homology in Archaeplastida suggests common ancestry of the  
263 heterodimerizing TALEs between Metazoa and Archaeplastida. It also predicted that other  
264 eukaryotic lineages might possess TALEs with the PBC-homology. Outside animals, the  
265 Pfam database contains only two PBC-B domain-harboring sequences, one from a  
266 Cryptophyta species (*Guillardia theta*, ID\_137502) and the other from an Amoebozoa  
267 species (*Acanthamoeba castellanii*, ID:XP\_004342337)[31]. We further examined the  
268 Excavata group, near to the posited root of eukaryotic phylogeny [22]. A search of two  
269 genomes (*Naegleria gruberi* and *Bodo saltans*) collected 12 TALE homeobox sequences in  
270 *N.gruberi*, and none in *B.saltans*, of which we found one with a PBC-homology domain  
271 (ID:78561, Fig 3A) and one with a MEIS/KNOX-homology (ID:79931, S2 Fig). Our data  
272 suggest that the heterodimerization domains -- the PBC-homology and MEIS/KNOX-  
273 homology -- originated early in eukaryotic evolution and persisted throughout the major  
274 eukaryotic radiations.

275



276 **Intron-retention supports the parallel evolution of the heterodimeric TALE classes**  
277 **during eukaryotic radiations**

278 The ubiquitous presence of dyadic TALEs raised next question: Are all the dyadic TALEs  
279 reported in this study the descendants of a single ancestral dyad, or do they result from  
280 lineage-specific evolution from a single prototypical TALE (proto-TALE) that does not  
281 engage in heterodimerization. To probe deep ancestry, we examined intron-retention, this  
282 being regarded as a long-preserved character and less prone to occur by homoplasy (a  
283 character displayed by a set of species but not present in their common ancestor) [32]. Five  
284 intron positions were shared by at least two TALE classes, of which the 44/45 and 48[2/3]  
285 introns qualified as the most ancestral since they were found throughout the Archaeplastida  
286 and Metazoa (S10 Fig).

287  
288 The 44/45 and 48[2/3] introns showed an intriguing exclusive distribution between the two  
289 dyadic partners of each phylum: one possesses the 44/45 and the other the 48[2/3] intron  
290 (S10 Fig). This mutually exclusive pattern suggested that two TALE genes with distinct  
291 intron positions existed at the onset of the eukaryotic radiation. We consider the 44/45 intron  
292 position as the most ancestral, given that it was conserved in most non-TALE homeobox  
293 genes [12]. In this regard, we speculate that acquisition of the 48[2/3], and loss of the 44/45  
294 intron, accompanied an early event wherein the proto-TALE with the 44/45 intron was  
295 duplicated to generate a second TALE with the 48[2/3] intron. Since the two intron positions  
296 were found within both the MEIS/KNOX and PBC/PBX/GLX groups, we propose that the  
297 duplicated TALEs arose early and diversified to establish lineage-specific heterodimeric  
298 configurations during eukaryotic radiations.

299  
300 Given that the heterodimeric TALEs evolved in a lineage-specific manner, we asked what  
301 the proto-TALE looked like at the time it underwent duplication. The following observations  
302 suggest that the proto-TALE was a homodimerizing protein. First, the PBC-homology  
303 domains of PBX/GLX class proteins identified in the Archaeplastida includes the MEINOX-  
304 motif that was originally defined for its similarity to the MEIS/KNOX-homology domains (Fig  
305 3) [14]. Second, PBX-Glaucoc sequences possess the ELK-homology within their PBL  
306 domain (Fig 3), which align well to the ELK domains of KNOX class sequences in  
307 Viridiplantae (S11 Fig). Therefore, the MEINOX-motif and ELK-homology across the  
308 heterodimerizing KNOX and PBX groups supported the common origin of heterodimerizing  
309 TALE groups from a single TALE by duplication followed by subfunctionalization.

310  
311 **Discussion**

312

### 313 **TALE endowment in Archaeplastida**

314 Our study shows that all three Archaeplastida phyla possess TALEs, diverged into two  
315 groups with distinct heterodimerization domains, the KNOX group with KN-A/KN-B domains  
316 and the PBX (or GLX) group with PBL domains. The similarity between the KNOX/PBX and  
317 the animal MEIS/PBC dyads led us to identify homologous heterodimerization domains in  
318 the TALEs of other eukaryotic lineages including Excavata. Based on our findings, we  
319 hypothesize that the TALE heterodimerization arose very early in eukaryotic evolution.

320

321 During > 1 BY of Archaeplastida history, TALE TF networks have undergone three  
322 duplication events compared to the simple dyadic TALEs in Glaucophyta. In Viridiplantae,  
323 the KNOX class persists as a single member throughout the mostly unicellular Chlorophyta,  
324 whereas it duplicated into KNOX1 and KNOX2 in the multicellular Streptophyta [33]. In  
325 Rhodophyta, two KNOX classes, KNOX-Red1 and KNOX-Red2 differ in KN-A and KN-B  
326 domains, suggesting sub-functionalization. The third duplication event occurred in the non-  
327 KNOX group of the Chlorophyta, whose sequences then underwent rapid divergence in their  
328 homeodomain and heterodimerization domains, rendering their classification trickier than  
329 other classes. Despite this divergence, proteins in one of the two radiations (Class-B and  
330 Mam-B) were found to heterodimerize with KNOX homologs, suggesting that these non-  
331 KNOX members serve as regulators of KNOX/GLX heterodimers. We summarize our finding  
332 in Fig 1, S10B Fig.

333

### 334 **Is the plant BELL class homologous to the Chlorophyta GLX class?**

335 The BELL class is the only non-KNOX class in land plants, sharing a POX (Pre-homeobox)  
336 domain (PF07526) [13] and lacking an identifiable PBL domain. The *K. flaccidum* genome,  
337 the only genome available in the charophyte lineage from which land plant emerged,  
338 contained three non-KNOX sequences, all possessing a PBL domain (Fig 3, S3,S4 Fig).  
339 Therefore, the lack of PBL-homology in the plant BELL class appears to be due to  
340 divergence or domain loss from an old charophyte class that had PBL-homology. We found  
341 an intron at the 24[2/3] homeodomain position of a *K. flaccidum* GLX homolog, which was  
342 previously identified as being specific to the plant BELL class (S8A Fig) [12], suggesting that  
343 the plant BELL class evolved from an ancestral GLX gene. More taxon sampling in  
344 charophytes is needed to confirm this inference.

345

### 346 **What would have been the critical drivers of TALE heterodimerization networks** 347 **emerging from ancestral homodimers?**

348 We found two conserved intron positions and shared sequence motifs between the KNOX-  
349 and PBX-groups, generating our hypothesis that a proto-TALE protein initially engaged in

350 homodimerization and then duplicated and diversified into two heterodimerizing classes (Fig  
351 1, S9A Fig). Heterodimerization-dependent subcellular localization [10,34], coupled with  
352 numerous combinations of distinct DNA-binding modules that fine-tune target specificity,  
353 then generated customized transcription-on switches.

354

355 During sexual development, it is critical to accurately detect the fusion of two cells before  
356 initiating diploid development and to make sure that the mating combines correct partner  
357 gametes. TF heterodimerization can implement both steps if one TF partner is contributed  
358 by each gamete. In fact, TALE heterodimerization plays a central role as a developmental  
359 switch for the haploid-to-diploid transition in green algae and land plants [10,19]. A similar  
360 haploid-to-diploid transition triggered by TF heterodimerization has recently been  
361 documented in *Dictyostelium* [35] and is well described in Basidiomycete fungi that utilize  
362 non-TALE homeobox proteins such as bW and bE [36,37].

363

364 Discovery of new prokaryotic life forms, especially in the Archaea domain, suggests that  
365 multiple symbiotic mergers of different life forms evolved into the proto-eukaryotes, possibly  
366 first as a symbiotic community, which then evolved into the last eukaryotic common  
367 ancestors (LECA) that rapidly diverged into the eukaryotic supergroups [38-40]. This  
368 eukaryogenesis model predicts that the proto-eukaryotes → LECA transition required the  
369 faithful transmission of traits between progenitor cells and their progeny to evolve as  
370 individual lineages by Darwinian selection. Under this hypothesis, we anticipate that the  
371 generation of the LECA may have been driven by the sexual mechanisms that distinguish a  
372 cellular merger between the common descendants from a merger between unrelated  
373 community members. Our proposal for the evolution of heterodimeric TALEs from the  
374 homodimeric proto-TALE may provide one of the necessary mechanisms for the first sexual  
375 mode of reproduction that might have driven the generation of the LECA from its proto-  
376 eukaryotic ancestors.

377

### 378 **Does expansion of heterodimerizing TALE TFs relate to the emergence of** 379 **multicellular complexity?**

380 Plant studies have shown that the duplicated KNOX classes serve distinct functions: the  
381 plant KNOX1 class regulates the differentiation of an undifferentiated cell mass into spores  
382 in mosses or leafy organs in vascular plants, and the plant KNOX2 class regulates the  
383 transition from haploid gametophytes to diploid sporophytes in mosses and controls  
384 secondary cell wall development in vascular plants [18,41-43]. We propose that the  
385 duplicated TALE heterodimers in the Streptophyta allowed independent regulation of cellular  
386 differentiation and life cycle transitions, priming the emergence of land plants by expanding

387 the diploid phase of their life cycle from a dormant zygospore to a multicellular individual  
388 bearing many meiotic spores. The repertoire of TALE heterodimers continued to expand  
389 during land plant evolution, serving all the major organ differentiation programs in the diploid  
390 phase of their life cycle.

391

392 Can a similar expansion of TALE heterodimers be found during Metazoan evolution? Our  
393 search for TALE TFs in unicellular relatives of the Metazoa -- Spingoeca and Monosiga --  
394 revealed a simple configuration with one MEIS- and one PBC-like TALE (S12, S13 Fig),  
395 whereas at the Metazoan base one finds at least three MEIS-related classes and two PBC-  
396 related classes [44]. These findings suggest the occurrence of a similar expansion of a  
397 founding dyad during Metazoan evolution. Therefore, in both plants and animals, the TALE  
398 TF network seems to be redeployed for complex multicellularity, departing from its posited  
399 original function in sexual development.

400

401 Our results suggest that TALE TF networks represent early-evolving developmental  
402 mechanisms. That said, the emergence of complex multicellularity doubtless required more  
403 than TF networks. TF-based developmental cues need to be propagated via chromatin-level  
404 regulatory mechanisms that establish the cellular memory during embryo development. The  
405 extent to which chromatin-level regulatory mechanisms are involved in the development of  
406 unicellular organisms is a critical question in elucidating the origins of complex  
407 multicellularity.

408

## 409 **Materials and methods**

### 410 **Strains and culture conditions**

411 Axenic *Micromonas commoda* (RCC299) and *Ostreococcus tauri* (OTH95) were maintained  
412 in Keller medium [45] in artificial seawater at room temperature. One hundred mL of a 14-  
413 day-old culture was harvested for genomic DNA extraction. *Picocystis salinarum*  
414 (CCMP1897) was obtained from the National Center for Marine Algae and Microbiota  
415 (NCMA), maintained in L1 medium [46] in artificial sea water, and plated on 1.5% Bactoagar-  
416 containing media for single-colony isolation. Genomic DNA of *P. salinarum* was then  
417 obtained from a culture derived from one colony.

418

### 419 **Phylogenetic analysis and classification of homeobox genes**

420 Archaeplastida algal TALE homeodomains were collected from the available genomes and  
421 transcriptomes listed in S1 Spreadsheet. Details of how TALE sequence was collected is  
422 provided in S1A Methods. After excluding nearly identical sequences, a total of 96  
423 sequences together with 18 reference TALE sequences were made into the final

424 homeodomain alignment with 70 unambiguously aligned positions with eight gapped and  
425 one constant sites. Details of phylogenetic reconstruction is provided in S1B Methods.

426

### 427 **Bioinformatics analysis**

428 The entire TALE collection was divided into multiple groups representing major clades in the  
429 homeodomain tree. Each group was individually analyzed by running MEME4.12 in the  
430 motif-discovery mode with default option collecting up to 10 motifs at <http://meme-suite.org/>  
431 [47]. The search provided multiple non-overlapping motifs, many of which were combined  
432 according to previously identified domains such as bipartite KN-A/KN-B, ELK, and HD [14]  
433 and independent domain searches against the INTERPRO database  
434 (<http://www.ebi.ac.uk/interpro/>) [48]. All the collected TALE-associated homology domains  
435 were aligned to generate HMM motifs, which we used to test if these homology domains are  
436 specific to the TALE sequences. All the homology domain information was used to locate  
437 any error in gene predictions, and gene models were updated if necessary (Details of the  
438 gene model curation is provided in S1C Methods).

439

### 440 **Intron comparison**

441 Introns within the homeodomain were collected and labeled as site numbers of the  
442 homeodomain (1-63). If an intron is between two codons it is denoted N/N+1, where N is the  
443 last amino acid site number of the preceding exon; introns within a codon are denoted  
444 N[n/n+1], where n is one or two for the codon nucleotide position relative to the splice-sites.

445

### 446 **Yeast-two-hybrid analysis**

447 *M. commoda* (affixed with Micco), *O. tauri* (affixed with Ostta), and *P. salinarum* (affixed with  
448 Picsa) TALE protein coding sequences were cloned by PCR using primers designed herein  
449 (S4 Spreadsheet) from genomic DNAs prepared by the phenol/chloroform extraction and  
450 ethanol precipitation method. Micco\_62153 and Picsa\_04684 contained a single intron,  
451 whereas all the other nine genes lacked an intron in the entire open reading frame. For  
452 cloning of Micco\_62153, we synthesized the middle fragment lacking the intron and ligated  
453 them via *Xho*I and *Cla*I sites. For cloning details, see S1D Methods.

454

### 455 **Supporting Information**

#### 456 **S1 Fig. Alignment of TALE homeodomain sequences of the Archae-algal collection.**

457 The 106 sequences were made into an alignment after excluding 20 near identical  
458 sequences to reduce redundancy. Animal/amoeba/haptophyte outgroup sequences are  
459 included as they share homology with Archaeplastida TALEs outside the homeodomain. The  
460 three bars above the sequence numbers show predicted alpha helices. Discarded insertions

461 are noted in red arrowheads.

462 **S2 Fig. Homology domain alignment of KNOX homologs.** MEIS class outgroup  
463 sequences are included at the bottom. Class label is on the left. KN-A, KN-B, ELK,  
464 HOMEBOX, KN-C1, and KN-C2 domains are labeled on the top. Class groups are labeled  
465 by colored bars on the left next to the gene names. Yellow, light green, and green shades in  
466 sequences show more than 60%, 80%, or 100% similarity in each column. Gaps between  
467 KN-A and KN-B and between KN-B and ELK have been eliminated.

468 **S3 Fig. GLX class is defined by PBL-Chloro domain.** (A-C) Three alignments are  
469 adjusted with inserting gaps for direct comparison among different PBL-Chloro domains. (A)  
470 GLX-Chloro class members. (B) GLX-Basal class members. (C) Three Viridiplantae  
471 sequences with strong MEINOX homology domain. PBC-homology is shared among the  
472 Chlorophyta non-KNOX sequences.

473 **S4 Fig. Extensive homology of Picsa\_04995 and Klefl\_00021\_0250 to Chocr\_41034**  
474 **indicates their classification as PBX-Red.** MEINOX-homology and PBL-Red domains are  
475 indicated by red bars below the alignment.

476 **S5 Fig. Alignment of Class-B TALE proteins in volvocales.** Short motifs are conserved  
477 among all members in this class over the entire length of the sequence.

478 **S6 Fig. Alignment of Mam-A TALE proteins in mamiellophyceae.** Short motifs (Box1-4)  
479 are conserved among all members in this class over the entire length of the sequence. Red  
480 reverse triangle at 548-549 shows the truncation position of Micco\_Mam-A-tr used in Yeast-  
481 two-hybrid analysis.

482 **S7 Fig. Alignment of Mam-B TALE proteins in mamiellophyceae.** A conserved motif is  
483 found between 180-197 amino acids in the alignment. Red reverse triangle at 100-101  
484 shows the truncation position of Ostta\_Mam-B-tr used in Yeast-two-hybrid analysis.  
485 Homology is restricted to a single homology-A domain outside the homeodomain.

486 **S8 Fig. Full-length proteins are necessary for mamiellophyceae non-KNOX TALE**  
487 **proteins to form heterodimers.** Left and Right: Yeast-two-hybrid assays on Ade-/His-/Leu-  
488 /Trp- medium. The construct information for the prey conjugated with the GAL4 DNA-binding  
489 domain and for the bait conjugated with the GAL4 transcriptional activation domain is given  
490 in the table below.

491 **S9 Fig. TALE interaction network defined by this study using yeast-two-hybrid**  
492 **assays.** (A) Summary diagram for the TALE interaction network. (B) Yeast-two-hybrid  
493 assays for the cross-species interaction of TALE proteins. Only one of the possible  
494 reciprocal combinations of GAL4 domain conjugations is provided for simplicity. Large X  
495 indicates no yeast in the sector. -LTHA: Leu-/Trp-/His-/Ade- medium; -LT: Leu-/Trp- medium.

496 **S10 Fig. Intron-retention pattern suggests parallel evolution of KNOX and non-KNOX**  
497 **group classes from common duplicated TALE ancestors.** (A) Intron locations collected

498 from 12 TALE classes are shown with arrows. Half arrows indicate cases where not all the  
499 class members share the position. White arrows indicate shared positions in at least two  
500 different classes, and black arrows indicate class-specific positions. The numbers above the  
501 consensus sequence show 60 amino acid positions; the three-amino-acid extension is  
502 denoted as 'abc.' Row color depicts two alternative domain configurations: purple for  
503 MEIS/KNOX types, and navy for PBX/GLX types. Class names are colored according to  
504 their phylogenetic groups: green for Viridiplantae, red for Rhodophyta, blue for Glaucophyta,  
505 and black for outgroups. The numbers following the class names show how many genes  
506 provided the intron information. Of the shared positions, purple triangles on the top mark  
507 those shared between MEIS/KNOX and PBX/GLX classes, blue triangles mark those shared  
508 between GLX and BELL classes, and red triangles mark those shared between KNOX  
509 classes. A notable exception is the KNOX-Red1 class, for which three Rhodophyta clades  
510 show different intron locations (44/45, 48[2/3] or 53[2/3]), indicating that the 44/45 intron  
511 position can indeed be displaced to 48[2/3] or elsewhere, albeit infrequently.-The unique  
512 46/47 intron in the PBX-Glauco (Cyapa\_20927) would presumably have resulted from a  
513 similar displacement in intron position. (B) Distribution of conserved introns among the TALE  
514 homeobox classes. Identified TALE classes are mapped on the Archaeplastida phylogeny.  
515 The 44/45 intron is marked by blue outline and the 48[2/3] intron is marked by red outline.  
516 Underlines of the class names indicate the presence of a PBC-homology domain. The  
517 Archaeplastida phylogeny is modified from figure 1 of Jackson et al. (2015).

518 **S11 Fig. ELK-domain alignment.**

519 **S12 Fig. Identification of MEIS homologs in choanoflagellates.**

520 **S13 Fig. Identification of PBX homologs in choanoflagellates.**

521

522 **S1 Spreadsheet Genomic resources used in this study.** A total of 374 homeobox protein  
523 sequences are compiled for this analysis, of which 113 TALE protein sequences are  
524 collected. The number of total homeobox proteins and TALE superclass were estimated  
525 largely from our homeodomain search described in the materials and methods section.  
526 Under Genome annotation, 'Draft' indicates a genome without annotation, 'Trans' indicates a  
527 transcriptome assembly.

528 **S2 Spreadsheet Archaeplastidal homeobox collection of TALE protein analyzed in**  
529 **this study.** For outgroups, only TALE members that are analyzed in this study are included.

530 **S3 Spreadsheet KNOX domain homology among KNOX classes**

531 **S4 Spreadsheet Primers used in this study**

532 **S5 Spreadsheet Yeast-two-hybrid constructs used in this study**

533 **S6 Spreadsheet Homeobox profile in Trebouxiophyceae**

534 **S1 Methods**

535 A. Collecting TALE homeobox protein sequences. B. Phylogenetic reconstruction. C.  
536 Homology motif/domain search. D. Intron comparison. E. Cloning of Yeast-two-hybrid  
537 constructs.

### 538 **S1 Notes**

539 A. Lack of TALE TFs in Trebouxiophyceae. B. Horizontal transfer may explain the presence  
540 of Rhodophyta TALE heterodimers in *Picocystis* and *Klebsormidium* of Viridiplantae.

541

### 542 **Acknowledgements**

543 This work was supported by Discovery Grant 418471-12 from the Natural Sciences and  
544 Engineering Research Council (NSERC) (to J.-H.L.), by the Korea CCS R&D Center  
545 (KCRC), Korean Ministry of Science, grant no. 2016M1A8A1925345 (to J.-H.L.), NSF-  
546 IOS0843119 (to A.Z.W.), GBMF 3788 (to A.Z.W.), and NSF CAREER-1453639  
547 (to E.K.). Postdoctoral support of S.J. was from NSF-IOS0843506 (awarded to Ursula  
548 W.Goodenough). We thank Mary Berbee and her laboratory members for valuable  
549 comments on the manuscript.

550

### 551 **Author Contributions**

552 **Conceptualization:** Sunjoo Joo, Alexandra Z. Worden, Jae-Hyeok Lee

553 **Data curation:** Sunjoo Joo, Ming Hsiu Wang, Gary Lui, Jenny Lee, Sebastian Sudek, Jae-  
554 Hyeok Lee

555 **Formal analysis:** Sunjoo Joo, Ming Hsiu Wang, Jae-Hyeok Lee

556 **Funding acquisition:** Sunjoo Joo, Alexandra Z. Worden, Jae-Hyeok Lee

557 **Investigation:** Sunjoo Joo, Ming Hsiu Wang, Jenny Lee, Andrew Barnas, Jae-Hyeok Lee

558 **Project administration:** Alexandra Z. Worden, Jae-Hyeok Lee

559 **Resources:** Sunjoo Joo, Ming Hsiu Wang, Eunsoo Kim, Sebastian Sudek

560 **Supervision:** Sunjoo Joo, Jae-Hyeok Lee

561 **Writing – original draft:** Sunjoo Joo, Ming Hsiu Wang, Jae-Hyeok Lee

562 **Writing – review & editing:** Sunjoo Joo, Eunsoo Kim, Alexandra Z. Worden, Jae-Hyeok  
563 Lee

564

### 565 **References**

566 1. Billeter M, Qian YQ, Otting G, Muller M, Gehring W, Wuthrich K. Determination of  
567 the nuclear magnetic resonance solution structure of an Antennapedia  
568 homeodomain-DNA complex. J Mol Biol. 1993;234: 1084–1093.  
569 doi:10.1006/jmbi.1993.1661



- 570 2. Azpiazu N, Morata G. Functional and regulatory interactions between Hox and  
571 extradenticle genes. *Genes & Development*. 1998;12: 261–273.
- 572 3. Hudry B, Thomas-Chollier M, Volovik Y, Duffraisse M, Dard A, Frank D, et al.  
573 Molecular insights into the origin of the Hox-TALE patterning system. *eLife*. 2014;3:  
574 e01939. doi:10.7554/eLife.01939
- 575 4. Hake S, Smith HMS, Holtan H, Magnani E, Mele G, Ramirez J. The role of KNOX  
576 genes in plant development. *Annu Rev Cell Dev Biol*. Annual Reviews; 2004;20:  
577 125–151. doi:10.1146/annurev.cellbio.20.031803.093824
- 578 5. Hay A, Tsiantis M. KNOX genes: versatile regulators of plant development and  
579 diversity. *Development*. 2010;137: 3153–3165. doi:10.1242/dev.030049
- 580 6. Berthelsen J, Kilstrup-Nielsen C, Blasi F, Mavilio F, Zappavigna V. The sub cellular  
581 localization of PBX1 and EXD proteins depends on nuclear import and export  
582 signals and is modulated by association with PREP1 and HTH. *Genes &*  
583 *Development*. 1999;13: 946–953.
- 584 7. Stevens KE, Mann RS. A balance between two nuclear localization sequences and  
585 a nuclear export sequence governs extradenticle subcellular localization. *Genetics*.  
586 *Genetics*; 2007;175: 1625–1636. doi:10.1534/genetics.106.066449
- 587 8. Bhatt AM, Etchells JP, Canales C, Lagodienko A, Dickinson H. VAAMANA--a  
588 BEL1-like homeodomain protein, interacts with KNOX proteins BP and STM and  
589 regulates inflorescence stem growth in Arabidopsis. *Gene*. 2004;328: 103–111.  
590 doi:10.1016/j.gene.2003.12.033
- 591 9. Smith HMS, Hake S. The Interaction of Two Homeobox Genes,  
592 BREVIPEDICELLUS and PENNYWISE, Regulates Internode Patterning in the  
593 Arabidopsis Inflorescence. *Plant Cell*. 2003;15: 1717–1727.
- 594 10. Lee J-H, Lin H, Joo S, Goodenough U. Early sexual origins of homeoprotein  
595 heterodimerization and evolution of the plant KNOX/BELL family. *Cell*. 2008;133:  
596 829–840. doi:10.1016/j.cell.2008.04.028
- 597 11. Noyes MB, Christensen RG, Wakabayashi A, Stormo GD, Brodsky MH, Wolfe SA.  
598 Analysis of homeodomain specificities allows the family-wide prediction of preferred  
599 recognition sites. *Cell*. 2008;133: 1277–1289. doi:10.1016/j.cell.2008.05.023
- 600 12. Bürglin TR. Analysis of TALE superclass homeobox genes (MEIS, PBC, KNOX,  
601 Iroquois, TGIF) reveals a novel domain conserved between plants and animals.  
602 *Nucleic Acids Research*. 1997;25: 4173–4180.
- 603 13. Bellaoui M, Pidkowich MS, Samach A, Kushalappa K, Kohalmi SE, Modrusan Z, et  
604 al. The Arabidopsis BELL1 and KNOX TALE homeodomain proteins interact  
605 through a domain conserved between plants and animals. *Plant Cell*. 2001;13:  
606 2455–2470. doi:10.1105/tpc.010161

- 607 14. Bürglin TR. The PBC domain contains a MEINOX domain: coevolution of Hox and  
608 TALE homeobox genes? *Dev Genes Evol.* 1998;208: 113–116.
- 609 15. Mukherjee K, Brocchieri L, Bürglin TR. A comprehensive classification and  
610 evolutionary analysis of plant homeobox genes. *Molecular Biology and Evolution.*  
611 2009;26: 2775–2794. doi:10.1093/molbev/msp201
- 612 16. Nishimura Y, Shikanai T, Nakamura S, Kawai-Yamada M, Uchimiya H. Gsp1  
613 triggers the sexual developmental program including inheritance of chloroplast  
614 DNA and mitochondrial DNA in *Chlamydomonas reinhardtii*. *Plant Cell.* 2012;24:  
615 2401–2414. doi:10.1105/tpc.112.097865
- 616 17. Joo S, Nishimura Y, Cronmiller E, Hong RH, Kariyawasam T, Wang MH, et al.  
617 Gene regulatory networks for the haploid-to-diploid transition of *Chlamydomonas*  
618 *reinhardtii*. *Plant Physiol.* 2017;175: 314–332. doi:10.1104/pp.17.00731
- 619 18. Sakakibara K, Ando S, Yip HK, Tamada Y, Hiwatashi Y, Murata T, et al. KNOX2  
620 Genes Regulate the Haploid-to-Diploid Morphological Transition in Land Plants.  
621 *Science.* 2013;339: 1067–1070. doi:10.1126/science.1230082
- 622 19. Horst NA, Katz A, Pereman I, Decker EL, Ohad N, Reski R. A single homeobox  
623 gene triggers phase transition, embryogenesis and asexual reproduction. *Nature*  
624 *Plants.* 2016;2: 15209. doi:10.1038/nplants.2015.209
- 625 20. Worden AZ, Lee JH, Mock T, Rouze P, Simmons MP, Aerts AL, et al. Green  
626 Evolution and Dynamic Adaptations Revealed by Genomes of the Marine  
627 Picoeukaryotes *Micromonas*. *Science.* 2009;324: 268–272.  
628 doi:10.1126/science.1167222
- 629 21. Archibald JM. Genomic perspectives on the birth and spread of plastids.  
630 *Proceedings of the National Academy of Sciences.* National Academy of Sciences;  
631 2015;112: 10147–10153. doi:10.1073/pnas.1421374112
- 632 22. Adl SM, Simpson AGB, Lane CE, Lukeš J, Bass D, Bowser SS, et al. The revised  
633 classification of eukaryotes. *J Eukaryot Microbiol.* 2012;59: 429–493.  
634 doi:10.1111/j.1550-7408.2012.00644.x
- 635 23. Worden AZ, Follows MJ, Giovannoni SJ, Wilken S, Zimmerman AE, Keeling PJ.  
636 Rethinking the marine carbon cycle: Factoring in the multifarious lifestyles of  
637 microbes. *Science.* 2015;347: 1257594–1257594. doi:10.1126/science.1257594
- 638 24. Guillou, Eikrem, Massana, Romari, Vaultot. Diversity of Picoplanktonic  
639 Prasinophytes Assessed by Direct Nuclear SSU rDNA Sequencing of  
640 Environmental Samples and Novel Isolates Retrieved from Oceanic and Coastal  
641 Marine Ecosystems. *Annals of Anatomy.* 2004;155: 22–22.  
642 doi:10.1078/143446104774199592

- 643 25. Lewis LA, McCourt RM. Green algae and the origin of land plants. *American*  
644 *Journal of Botany*. 2004;91: 1535–1556. doi:10.3732/ajb.91.10.1535
- 645 26. Yoon HS, Muller KM, Sheath RG, Ott FD, Bhattacharya D. Defining the major  
646 lineages of red algae (RHODOPHYTA). *Journal of Phycology*. 2006;42: 482–492.  
647 doi:10.1111/j.1529-8817.2006.00210.x
- 648 27. Jackson C, Clayden S, Reyes-Prieto A. The Glaucophyta: the blue-green plants in  
649 a nutshell. *Acta Societatis Botanicorum Poloniae*. 2015;84: 149–165.  
650 doi:10.5586/asbp.2015.020
- 651 28. Bertolino E, Reimund B, Wildt-Perinic D, Clerc RG. A novel homeobox protein  
652 which recognizes a TGT core and functionally interferes with a retinoid-responsive  
653 motif. *J Biol Chem*. 1995;270: 31178–31188.
- 654 29. Kurvari V, Grishin NV, Snell WJ. A gamete-specific, sex-limited homeodomain  
655 protein in *Chlamydomonas*. *J Cell Biol*. 1998;143: 1971–1980.
- 656 30. Piganeau G, Grimsley N, Moreau H. Genome diversity in the smallest marine  
657 photosynthetic eukaryotes. *Res Microbiol*. 2011;162: 570–577.  
658 doi:10.1016/j.resmic.2011.04.005
- 659 31. Clarke M, Lohan AJ, Liu B, Lagkouvardos I, Roy S, Zafar N, et al. Genome of  
660 *Acanthamoeba castellanii* highlights extensive lateral gene transfer and early  
661 evolution of tyrosine kinase signaling. *Genome Biology*. 2013;14: R11.  
662 doi:10.1186/gb-2013-14-2-r11
- 663 32. Sverdlov AV, Rogozin IB, Babenko VN, Koonin EV. Conservation versus parallel  
664 gains in intron evolution. *Nucleic Acids Research*. 2005;33: 1741–1748.  
665 doi:10.1093/nar/gki316
- 666 33. Frangedakis E, Saint-Marcoux D, Moody LA, Rabbinowitsch E, Langdale JA.  
667 Nonreciprocal complementation of KNOX gene function in land plants. *The New*  
668 *phytologist*. 2016;341: 95–604. doi:10.1111/nph.14318
- 669 34. Longobardi E, Penkov D, Mateos D, De Florian G, Torres M, Blasi F. Biochemistry  
670 of the tale transcription factors PREP, MEIS, and PBX in vertebrates. Wellik D,  
671 Torres M, Ros M, editors. *Dev Dyn*. 2014;243: 59–75. doi:10.1002/dvdy.24016
- 672 35. Hedgethorpe K, Eustermann S, Yang J-C, Ogden TEH, Neuhaus D, Bloomfield G.  
673 Homeodomain-like DNA binding proteins control the haploid-to-diploid transition  
674 in *Dictyostelium*. *Science Advances*. 2017;3: e1602937.  
675 doi:10.1126/sciadv.1602937
- 676 36. Kües U, Asante-Owusu RN, Mutasa ES, Tymon AM, Pardo EH, O'Shea SF, et al.  
677 Two classes of homeodomain proteins specify the multiple mating types of the  
678 mushroom *Coprinus cinereus*. *Plant Cell*. 1994;6: 1467–1475.  
679 doi:10.1105/tpc.6.10.1467

- 680 37. Spit A, Hyland RH, Mellor EJC, Casselton LA. A role for heterodimerization in  
681 nuclear localization of a homeodomain protein. *Proc Natl Acad Sci USA*. 1998;95:  
682 6228–6233. doi:10.1073/pnas.95.11.6228
- 683 38. O'Malley MA. Endosymbiosis and its implications for evolutionary theory. *Proc Natl*  
684 *Acad Sci USA*. 2015;112: 10270–10277. doi:10.1073/pnas.1421389112
- 685 39. López-García P, Eme L, Moreira D. Symbiosis in eukaryotic evolution. *Journal of*  
686 *Theoretical Biology*. 2017;434: 20–33. doi:10.1016/j.jtbi.2017.02.031
- 687 40. Zaremba-Niedzwiedzka K, Caceres EF, Saw JH, Bäckström D, Juzokaite L,  
688 Vancaester E, et al. Asgard archaea illuminate the origin of eukaryotic cellular  
689 complexity. *Nature*. 2017;541: 353–358. doi:10.1038/nature21031
- 690 41. Barton MK, Poethig RS. Formation of the shoot apical meristem in *Arabidopsis*  
691 *thaliana*: an analysis of development in the wild type and in the shoot meristemless  
692 mutant. *Development*. 1993;119: 823–831.
- 693 42. Li E, Bhargava A, Qiang W, Friedmann MC, Forneris N, Savidge RA, et al. The  
694 Class II KNOX gene *KNAT7* negatively regulates secondary wall formation in  
695 *Arabidopsis* and is functionally conserved in *Populus*. *The New phytologist*.  
696 2012;194: 102–115. doi:10.1111/j.1469-8137.2011.04016.x
- 697 43. Furumizu C, Alvarez JP, Sakakibara K, Bowman JL. Antagonistic roles for *KNOX1*  
698 and *KNOX2* genes in patterning the land plant body plan following an ancient gene  
699 duplication. Qu L-J, editor. *PLoS Genet*. 2015;11: e1004980.  
700 doi:10.1371/journal.pgen.1004980
- 701 44. Mukherjee K, Bürglin TR. Comprehensive analysis of animal TALE homeobox  
702 genes: new conserved motifs and cases of accelerated evolution. *J Mol Evol*.  
703 2007;65: 137–153. doi:10.1007/s00239-006-0023-0
- 704 45. Keller MD, Selvin RC, Claus W, Guillard RRL. MEDIA FOR THE CULTURE OF  
705 OCEANIC ULTRAPHYTOPLANKTON1,2. *Journal of Phycology*. 2007;23: 633–  
706 638. doi:10.1111/j.1529-8817.1987.tb04217.x
- 707 46. Guillard RRL, Hargraves PE. *Stichochrysis immobilis* is a diatom, not a  
708 chrysophyte. *Phycologia*. 1993;32: 234–236. doi:10.2216/i0031-8884-32-3-234.1
- 709 47. Bailey TL, Johnson J, Grant CE, Noble WS. The MEME Suite. *Nucleic Acids*  
710 *Research*. 2015;43: W39–49. doi:10.1093/nar/gkv416
- 711 48. Finn RD, Attwood TK, Babbitt PC, Bateman A, Bork P, Bridge AJ, et al. InterPro in  
712 2017-beyond protein family and domain annotations. *Nucleic Acids Research*.  
713 2017;45: D190–D199. doi:10.1093/nar/gkw1107

714

## 715 **Figure Legends**

716

717 **Fig 1. Common origin of heterodimerizing TALE homeobox TFs.** Hypothesized  
718 homodimerizing proto-TALE protein (top) duplicated before the eukaryotic radiations into  
719 animals/fungi/amoebae vs. algae/plants. Lineage-specific diversification soon followed,  
720 generating heterodimeric configurations distinct at the phylum-level. (Left) Each lineage  
721 possesses one or two classes of potential heterodimeric TALEs, which are summarized onto  
722 the eukaryotic phylogeny. A representative species name is given for each analyzed lineage.  
723 (Right) Summary of TALE configurations, coupling members of the PBC/PBX/GLX group  
724 that shares PBC-homology domains and of the MEIS/KNOX group that shows homology in  
725 the KN-A/B domains N-terminal to the homeodomain. Lightly shaded boxes depict homology  
726 domains, whose names are provided above. Open areas in the domain boxes indicate the  
727 absence of MEINOX-motif for PBX-Red, KN-A for KNOX-Red1 and ELK for KNOX-Red2.  
728 Colored vertical lines in the HD indicate two shared introns at 44/45 (orange over 'H' in HD)  
729 and 48[2/3] (blue over 'D' in HD), whose alternating existence between the two groups  
730 suggests independent diversification of TALE heterodimerization. HD: Homeodomain; PBL-  
731 C: PBL-Chloro; PBL-R: PBL-Red.

732

733 **Fig 2. Maximum likelihood (ML) phylogeny of the TALE superclass homeodomain in**  
734 **Archaeplastida supports ancient division between KNOX- and non-KNOX TALE**  
735 **groups.** The consensus tree out of 1000 bootstrap trees is shown. The three numbers at  
736 critical nodes show %bootstrap, %SH, and Bayesian posterior probability in support of  
737 clades. The tree contains two outgroup clades marked by black squares at nodes, and two  
738 Archaeplastida clades, one combining most KNOX sequences marked by the red square  
739 and the other combining all non-KNOX sequences marked by the blue square. Vertical bars  
740 on the right depict the distribution of outgroup in black, KNOX in red, and non-KNOX  
741 sequences in blue. Red dots by the sequence names indicate the presence of KN-A or KN-B  
742 domains, and blue dots indicate the presence of a PBC-homology domain. Truncated  
743 sequences not available for homology domain analysis are marked with open black boxes.  
744 Filled black boxes indicate the absence of a KN-A/B or PBC-homology domain. Proposed  
745 classification is indicated by the vertical lines. Dotted vertical lines indicate suggested class  
746 members placed outside the main clade for the class in the phylogeny. PBX-Red sequences  
747 are found in four separate clades, marked by purple shades on the blue section of the  
748 vertical bars. Colors of the sequence names indicate their phylogenetic group: Blue for  
749 Glaucophyta, purple for Rhodophyta, green for prasinophytes, light blue for the  
750 chlorophytes, orange for Streptophyta, and black for outgroups. The ruler shows genetic  
751 distance. Details of the sequences analyzed by this phylogeny are provided in S2  
752 Spreadsheet.

753

754 **Fig 3. Archaeplastida non-KNOX group TALEs possess a PBC-like domain (PBL)**  
755 **consisting of N-terminal MEINOX homology and C-terminal PBC-B homology.** Amino  
756 acid letters in black with gray shades, in white with light shades, and in white with black  
757 shades show more than 60%, 80%, or 100% similarity in each column. Inverse red triangles  
758 indicate the discarded sequences in un-aligned insertions. (A) PBL-Glauco domain  
759 alignment, including two Glaucophyta sequences sharing homology in both MEINOX  
760 homology and C-terminal half of the PBC-B domain with non-Archaeplastida TALE  
761 sequences. Red box indicates the ELK domain. (B) PBL-Red domain alignment. All  
762 Rhodophyta non-KNOX sequences possess a PBL domain with poor MEINOX homology.  
763 (C) PBL-Chloro domain alignment. *Cyanophora\_paradox\_20927.63* is included for  
764 comparison. *Picocystis\_salinarum\_02499* is a founding member of GLX class with a PBL-  
765 Chloro domain. (D) Comparison among PBL domains. The top row shows the consensus  
766 made from the alignment of (A), (B), and (C) combined and the lower consensus sequences  
767 are collected from the individual alignments presented in (A), (B), and (C).

768

769 **Fig 4. TALE TFs engage in heterodimerization networks between KNOX and non-**  
770 **KNOX groups.** The bait constructs conjugated to the GAL4 DNA-binding domain (DBD) and  
771 the prey constructs conjugated to the GAL4 transcriptional activation domain (AD) are listed  
772 in the table. Construct combinations, numbered 1-8, are arranged in wedges clock-wise,  
773 starting at 9 o'clock as labeled in the -LT panels. Confirmed interacting pairs are shown in  
774 bold faces in the table. The laminin and T-Antigen (T-Ag) pair, known to be interacting  
775 partners, was plated in the 8th sector as a positive control. (A) Assays using *M. commoda*  
776 TALEs. (B) Assays using *O. tauri* TALEs. (C) Assays using *P. salinarum* TALEs. KNOX-tr  
777 refers to the N-terminal truncated KNOX construct for preventing self-activation. (D)  
778 Detailed construct information is provided in S5 Spreadsheet.

779

1 **Figures for Joo et al.**

2 Article title: Common ancestry of heterodimerizing TALE homeobox transcription factors across  
3 Metazoa and Archaeplastida.

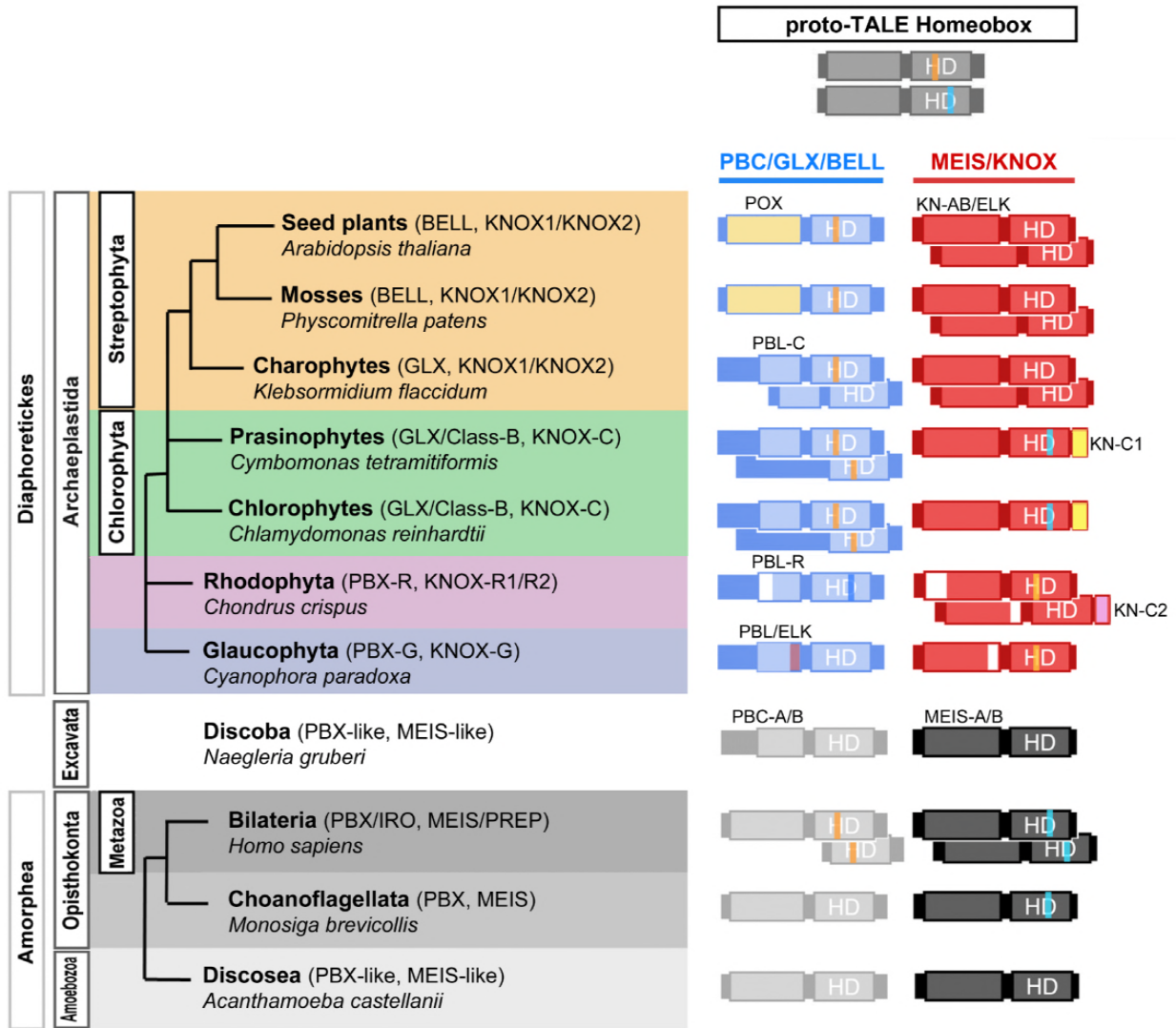
4 Authors: Sunjoo Joo, Ming Hsiu Wang, Gary Lui, Jenny Lee, Andrew Barnas, Eunsoo Kim,  
5 Sebastian Sudek, Alexandra Z. Worden, and Jae-Hyeok Lee.

6

7

8

9 Fig 1.



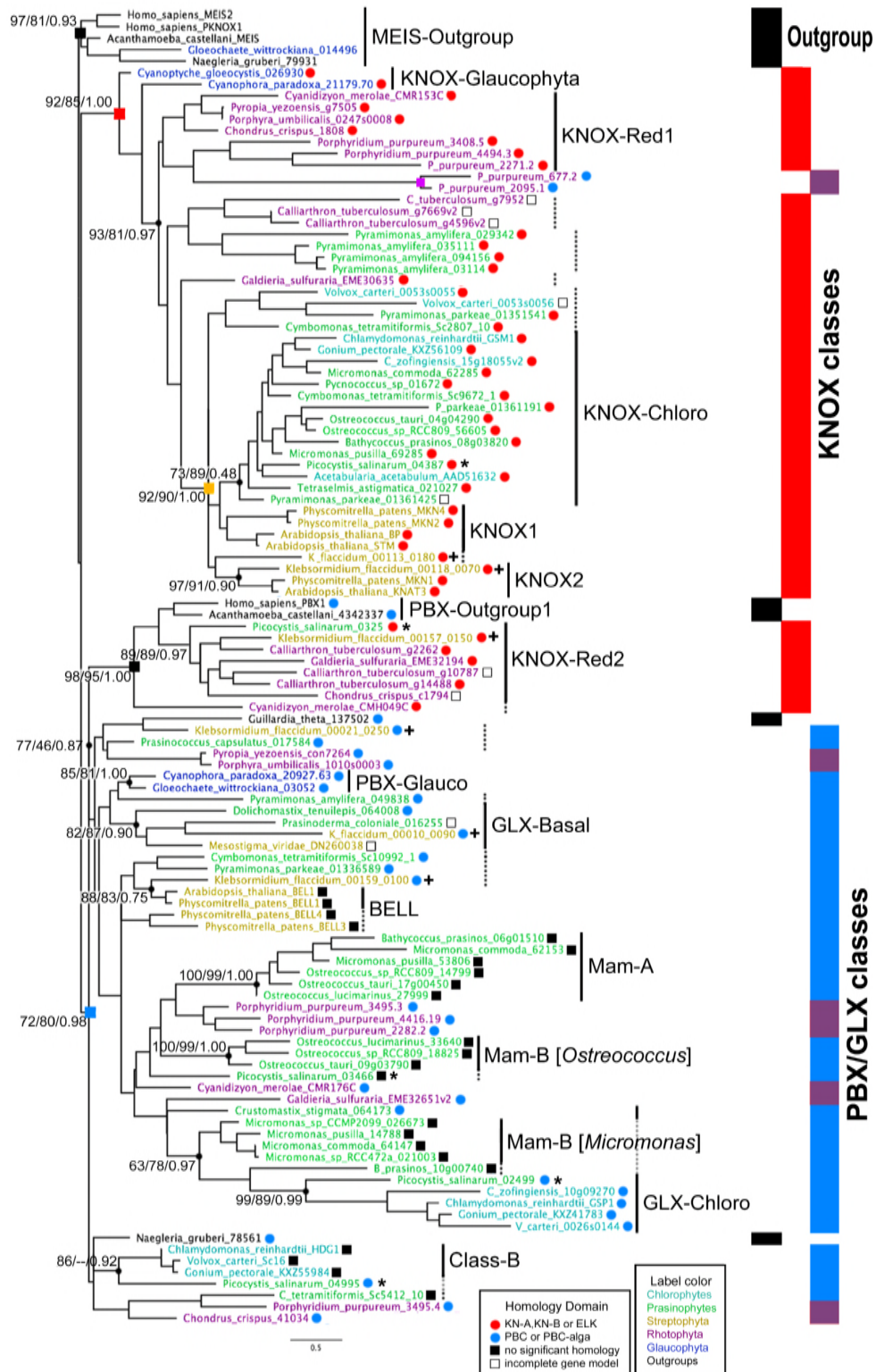
10

11 **Fig 1. Common origin of heterodimerizing TALE homeobox TFs.** We propose that a homodimerizing  
 12 proto-TALE protein duplicated (top) prior to the major bifurcation resulting in animals/fungi/amoebae vs.  
 13 algae/plants. Lineage-specific diversification soon followed, generating heterodimeric configurations  
 14 distinct at the phylum-level. These configurations usually couple members of the PBC/PBX/GLX group  
 15 that shares PBC-homology domains and MEIS/KNOX group that shows homology in the KN-A/B domains  
 16 N-terminal to the homeodomain. Each lineage possesses one or two classes of potential heterodimeric  
 17 partners. Major TALE classes are mapped onto the eukaryotic phylogeny. A representative species name  
 18 is given for each analyzed lineage. Open boxes in the domain diagrams indicate the absence of MEINOX  
 19 for PBX-Red, KN-A for KNOX-Red1 and ELK for KNOX-Red2. Colored vertical lines in the HD indicate  
 20 two proposed ancestral introns at 44/45 (orange over 'H' in HD) and 48[2/3] (blue over 'D' in HD), whose  
 21 alternating existence between the two groups suggests independent diversification of TALE  
 22 heterodimerization.

23



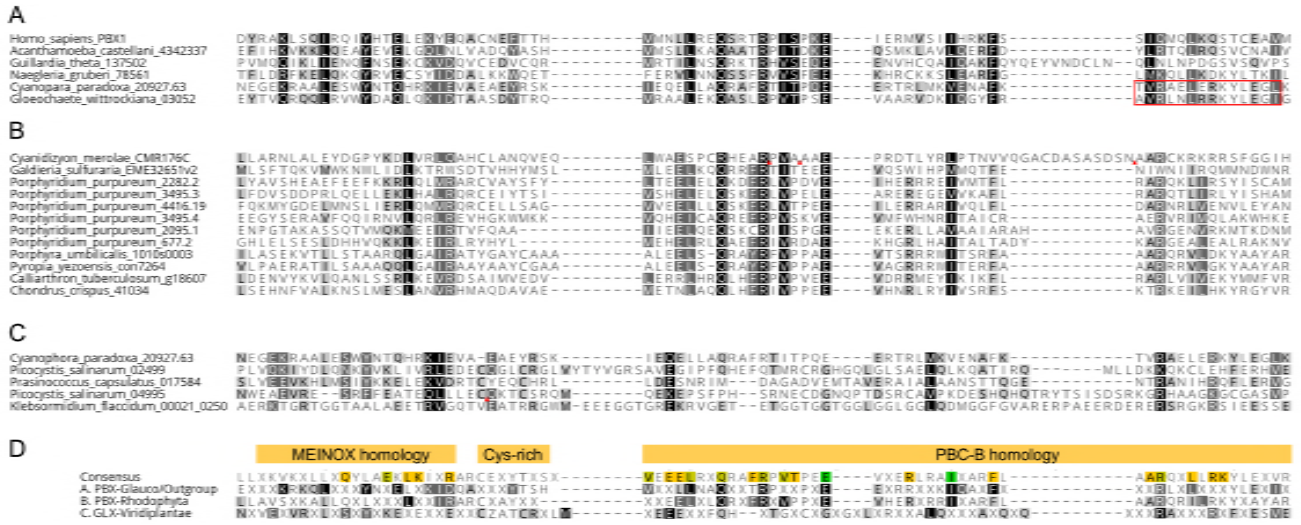
24 **Fig 2. Maximum likelihood (ML) phylogeny of the TALE superclass homeodomain in**  
 25 **Archaeplastida supports ancient division between KNOX- and non-KNOX TALE groups.**



27 **Fig 2. Maximum likelihood (ML) phylogeny of the TALE superclass HD in Archaeplastida supports**  
28 **ancient division between KNOX- and non-KNOX TALE groups.** The consensus tree out of 1000  
29 bootstrap trees is shown. The three numbers shown at nodes are %bootstrap, %SH, and Bayesian  
30 posterior probability in support of clades. The tree contains two outgroup clades marked by black  
31 squares, and two Archaeplastida clades, one combining most KNOX sequences marked by the red  
32 square and the other combining all non-KNOX sequences marked by the blue square. Vertical bars on  
33 the right depict the distribution of outgroup, KNOX, and non-KNOX sequences. KNOX sequences are  
34 marked with red dots indicating the presence of KN-A or KN-B domains. GLX/PBX sequences are  
35 marked with blue dots indicating the presence of a PBC-homology domain. Truncated sequences not  
36 available for homology domain analysis are marked with open black boxes. Filled box indicates the  
37 absence of a KN-A/B or PBC-homology domain. Proposed classification is shown by black vertical lines.  
38 Dotted lines indicate sequences related to a class but placed outside the main clade for the class. PBX-  
39 Red sequences are found in four paraphyletic clades, marked by purple shades on the blue vertical bar.  
40 Sequence IDs containing the species name are colored by their phylogeny: Blue for Glaucophyta, purple  
41 for Rhodophyta, green for prasinophytes, light blue for the chlorophytes, orange for Streptophyta, and  
42 black for outgroups. The ruler shows genetic distance. All the sequences and their phylogenetic  
43 information are found in S2 Spreadsheet.  
44  
45 \*Gloeochaete\_wittrockiana\_014496 is considered as a sequence from a bannelid-type amoeba that  
46 contaminated the original culture (SAG46.84) for the MMETSP1089 transcriptome. \*\*Association of  
47 KNOX-Red2 class sequences to Amorphea PBC sequences is attributed to a shared WFGN motif  
48 determining DNA-binding specificity of the homeodomain via convergent evolution.  
49

50

51 **Fig 3.**



52

53

54

55

56

57

58

59

60

61

62

63

64

65

66

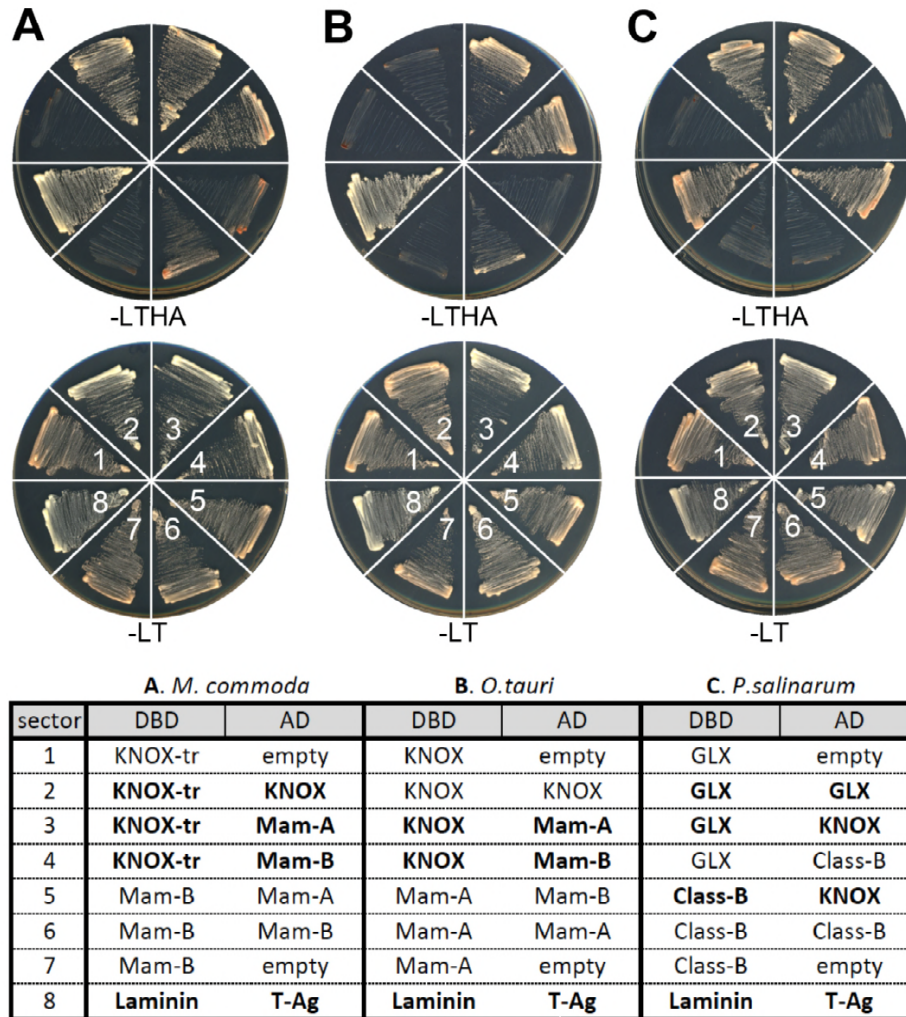
67

68

69

**Fig 3. Archaeplastida Non-KNOX group TALEs possess a PBL domain sharing homology with metazoan PBC class TALEs.** (A) PBL-Glauco domain alignment. Two Glaucophyta non-KNOX sequences possess a PBC-homology domain spanning MEINOX and C-terminal half of the PBC-B domains which is shared among the three outgroup TALE sequences analyzed in this study. (B) PBL-Red domain alignment. All Rhodophyta non-KNOX sequences possess a PBC-homology domain that can be aligned to the MEINOX/PBC-C domains. (C) PBL-Chloro domain. Four non-KNOX sequences show >10% amino acid identity to one of the other PBC-homology blocks presented in (A) and (B). Picocystis\_salinarum\_02499 is a founding member of GLX class with a PBL-Chloro domain. **D.** Comparison among PBC-homology domains. The top row shows the consensus made from the alignment of (A), (B), and (C) combined and the lower consensus sequences are collected from the individual alignments presented in (A), (B), and GLX alignment (S3 Fig). Amino acid letters in black with Gray shades, in white with light shades, and in white with black shades show more than 60%, 80%, or 100% similarity in each column.

70 Fig 4.



71

72

73 **Fig 4. All Chlorophyta TALE TFs engage in heterodimerization networks.** The bait constructs  
 74 conjugated to the GAL4 DNA-binding domain and the prey constructs conjugated to the GAL4  
 75 transcriptional activation domain are listed in the table. Construct combinations, numbered 1-8,  
 76 are arranged in wedges clock-wise, starting at 9 o'clock as labeled in (A). Interacting pairs confer yeast  
 77 growth in Leu-/Trp-/His-/Ade- (-LTHA) medium. Confirmed interacting pairs are shown in bold faces in the  
 78 table. The laminin and T-Antigen (T-Ag) pair, known to be interacting partners, was plated in the 8th  
 79 sector as a positive control. (A) Assays using *M. commoda* TALEs. (B) Assays using *O. tauri* TALEs. (C)  
 80 Assays using *P. salinarum* TALEs. Class-A refers to the GLX-Chloro homolog. Details of the construct  
 81 information are found in S5 Spreadsheet.

82

83